Analyst

Cite this: *Analyst*, 2011, **136**, 702

www.rsc.org/analyst

PAPER

A sensitive fluorimetric biosensor for detection of DNA hybridization based on Fe/Au core/shell nanoparticles

Yuzhong Zhang,* Zhen Wang and Wei Jiang

Received 28th July 2010, Accepted 10th November 2010
DOI: 10.1039/c0an00583e

In this study, we reported a sensitive fluorescent biosensor for detection of DNA hybridization based on Fe/Au core/shell (Fe@Au) nanoparticles (NPs). First, Fe@Au NPs were synthesized using a reverse micelle method, with gold as the shell and iron as the core. The nanoparticle size was confirmed by transmission electron microscopy (TEM). Scanning electron microscopy (SEM) was performed in order to elucidate the morphology of the Fe@Au NPs. Then probe DNA with –SH at the 5′-phosphate end was covalently immobilized onto the surface of the Fe@Au NPs. The DNA hybridization event can be detected by a fluorescent method and methylene blue (MB) as the fluorescent probe. The decline of the fluorescence intensity of MB (ΔF) was linear with the concentration of the complementary DNA from 3.0×10^{-13} to 1.0×10^{-9} M with a detection limit of 1.0×10^{-13} M (S/N = 3). In addition, this approach of DNA detection exhibited excellent selectivity, even for single-mismatched DNA detection.

Introduction

In recent years, the detection of DNA sequences has become more and more important in gene therapy, criminology, food safety, and a variety of biomedical studies.[1–3] Various techniques have been developed for DNA detection, such as electrochemical methods[4,5] and optical methods.[6–8] Among these protocols, fluorescence technology is known as a powerful tool because of its high sensitivity, good selectivity and easy operation. To date, some methods for the detection of DNA hybridization based on a fluorimetric technique have been reported.[9–11] As it is well known, the sensitivity of DNA detection can be improved using signal amplification, and most signal amplification strategies are performed by nanomaterials, such as nanoparticles and carbon nanotubes.[12–14] Among these nanomaterials, magnetic nanoparticles are attractive because they have good biocompatibility and can be separated very readily from reaction mixtures using an external magnetic field.[15,16] They have also been widely applied in the field of DNA hybridization detection.[17,18] For example, magnetic beads-based and gold nanoparticles-modified magnetic nanoparticles sensing methods have been developed.[19,20]

It is reported that a hybridization-in-solution format has faster kinetics than that on microarrays and electrodes.[21] The unbound probe DNA and the non-hybridized target DNA can be separated from solution with an external magnetic field. Hence this kind of hybridization format has been widely applied for molecular beacon hybridization,[22] and magnetic capture hybridization.[23,24] Hristova and co-workers reported a non-PCR1-based DNA hybridization-in-solution system using luminescent and magnetic lanthanide oxide nanoparticles.[25] Kouassi and co-workers developed a sensitive DNA fluorescence sensor based on magnetic nanoparticles.[26]

In this work, we reported a sensitive fluorescence biosensor for the detection of the target DNA using the hybridization-in-solution method. First, Fe@Au NPs were synthesized, and then the probe DNA with a mercapto group at the 5′-phosphate end was directly immobilized onto the Fe@Au NPs. The DNA hybridization event was monitored by a fluorescence technique and methylene blue (MB) as the fluorescence probe. As MB is a member of the phenothiazine family, it could bind to the single stranded DNA (ssDNA) by it specially reacting with guanine bases. When ssDNA was hybridized with target DNA to form double stranded DNA (dsDNA), MB cannot access them forming the MB–guanine base compound.[27,28] Therefore, we could use the decline of fluorescence intensity of MB during DNA hybridization to detect the concentration of target DNA. The experimental results showed that the proposed method exhibited excellent sensitivity and selectivity.

Experimental

Chemicals and reagents

Tris-(hydroxymethyl)aminomethane (Tris-base) was purchased from Alfa Aesar (Tianjing, China). Chloroauric acid ($HAuCl_4 \cdot 4H_2O$) was obtained from Shanghai Chemical Reagent Co., Ltd. Sodium hydroxide and hydrochloric acid were obtained from Nanjing Chemical Reagent (Nanjing, China).

College of Chemistry and Materials Science, Anhui Key Laboratory of Chemo-Biosensing, Anhui Normal University, Wuhu 241000, People's Republic of China. E-mail: zhyz65@mail.ahnu.edu.cn; Fax: +86 553 3869303; Tel: +86 553 3869303

Cetyltrimethylammonium bromide (CTAB), n-butanol, n-octane, ferrous sulfate ($FeSO_4$), and sodium borohydride ($NaBH_4$) were purchased from Sinopharm Chemical Reagent Co., Ltd (Shanghai, China). Methylene blue was purchased from the Third Reagent Factory of Shanghai. All DNA used in this work was purchased from Shanghai Sangon Bioengineering Technology & Services Co., Ltd (Shanghai, China). Their base sequences are shown as follows:

Probe sequence: 5′-SH-$(CH_2)_6$-GAG CGG CGC AAC ATT TCA GGT CGA-3′

Complementary sequence: 5′-TCG ACC TGA AAT GTT GCG CCG CTC-3′

Non-complementary sequence: 5′-AGC TGG ACT TTA CAA CGC GGC GAG-3′

One-base mismatched sequence: 5′-TCG ACC TGA AAC GTT GCG CCG CTC-3′.

All oligonucleotides stock solutions were prepared with 0.01 M Tris-HCl (pH 7.40) and kept frozen until used. The following buffer solutions were used: hybridization buffer solution (0.20 M NaCl + 0.01 M Tris-HCl, pH 7.40); detection buffer solution (0.01 M Tris-HCl, pH 7.40). All chemicals were of analytical grade and used without further purification. All solutions were prepared with twice-quartz-distilled water.

Instruments

All fluorescence measurements were performed on an F-4500 Fluorescence Spectrophotometer (Hitachi, Japan). The size of the Fe NPs and Fe@Au NPs was measured with transmission electron microscope (TEM) (Hitachi-800). The morphology of the Fe NPs and Fe@Au NPs was investigated by scanning electron microscopy (SEM) using a JEOLJSM-6700F microscope (Hitachi, Japan). The phase and crystallography of the products were identified by X-ray diffraction (XRD) equipped with high-intensity Cu Kλ radiation ($\lambda = 0.15406$ nm). A scanning rate of 0.05°/s was applied to record the pattern in the two theta range from 20° to 70°.

Synthesis of Fe@Au NPs and functionalized with DNA probe

Fe@Au NPs were synthesized according to the literature report.[29] Fe@Au NPs were prepared in a reverse micelle of cetyltrimethylammonium bromide (CTAB) using 1-butanol as a co-surfactant and octane as the oil phase. Briefly, 1.5 mL of 0.50 M $FeSO_4$(aq), 3.5 g of CTAB, 3.0 g of butanol, and 9.0 g of octane were mixed with 1.5 mL of 1.00 M $NaBH_4$(aq), 3.5 g of CTAB, 3.0 g of butanol, and 9.0 g of octane. Next the mixture was heated up to 60 °C with vigorous stirring for 20 min. Then 1.2 mL of 0.44 M $HAuCl_4$(aq), 1.8 g of CTAB, 1.5 g of butanol, and 0.6 g of octane along with 1.20 M $NaBH_4$(aq), 1.8 g of CTAB, 1.5 g of butanol, and 6.0 g of octane were added. The pH value was controlled at 11.00 and reacted for another 15 min. The Fe@Au NPs were washed with methanol and water three times and dried under vacuum.

1.0 OD of 5′-SH capped probe DNA were added into 5.0 mL of 10.0 mg mL^{-1} Fe@Au NPs suspended solution, and the suspension was gently stirred for 24 h. Unbound probe DNA was separated from the suspension using a magnet under the cell and washed with water and 0.01 M Tris-HCl solution three times. Fe@Au NPs functionalized with DNA probe were re-dispersed in 5.0 mL of Tris-HCl solution (pH 7.40) and stored at 4 °C in a fridge.

Hybridization and fluorescence detection

The DNA hybridization experiment was carried out by incubating 50 μL of the suspension of probe DNA functionalized nanoparticles with different concentrations of target oligonucleotide in 0.01 M Tris-HCl and 0.20 M NaCl solution for 30 min at 37 °C by gently stirring. When the DNA hybridization reaction was completed, the Fe@Au NPs were separated and washed with water and 0.01 M Tris-HCl three times to remove non-hybridized oligonucleotide. Then 2.0 mL of 1.0×10^{-5} M MB was added and incubated for 20 min. After the Fe@Au NPs were separated, it was washed with water and 0.01 M Tris-HCl three times to remove the excess MB. In the end, the Fe@Au NPs were suspended in 2.5mL of 0.01 M Tris-HCl. The fluorescence detection of the DNA hybridization was performed at excitation and emission wavelengths of 630 nm and 690 nm, respectively. And the concentration of complementary DNA was quantified by the decrease of MB fluorescence intensity before and after DNA hybridization ($\Delta F = F_{\text{ss-DNA}} - F_{\text{ds-DNA}}$). The principle of our method (including the probe DNA immobilization, hybridization and detection of complementary DNA) is described in Scheme 1.

Results and discussion

Characterization of Fe@Au NPs

Fig. 1 shows the XRD patterns of the Fe@Au NPs. All the peaks obtained are in good agreement with the known diffraction peaks for Fe@Au NPs from the literature reported,[29] which indicated that the nanoparticles were Fe@Au NPs. Also the shape and size of the nanoparticles were characterized by SEM and TEM. From the SEM images (Fig. 2), it is clearly observed that Fe@Au NPs (Fig. 2B, diameter: 50 nm) are larger than Fe NPs (Fig. 2A, diameter: 45 nm). The TEM images of Fe and Fe@Au NPs are shown in Fig. 2C and Fig. 2D, indicting that the Fe@Au NPs had a gold shell.

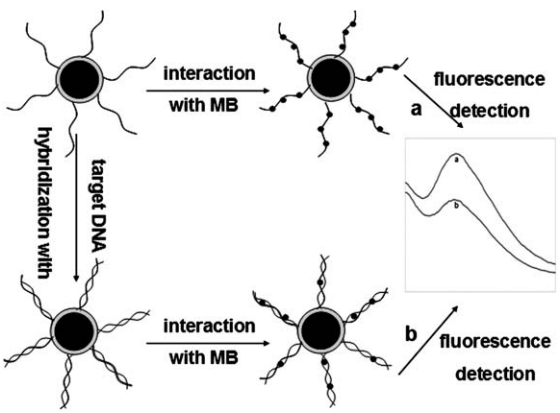

Scheme 1 Schematic representation of the procedure for DNA hybridization detection.

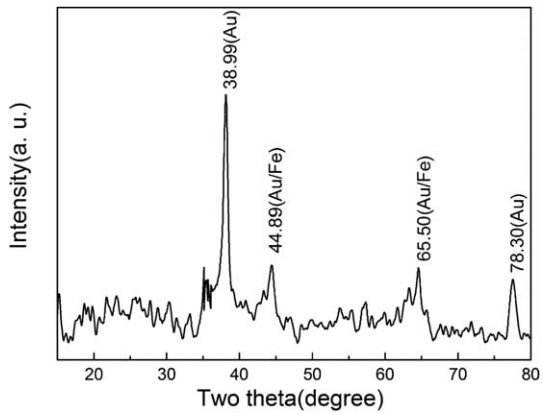

Fig. 1 The XRD pattern of the Fe@Au NPs.

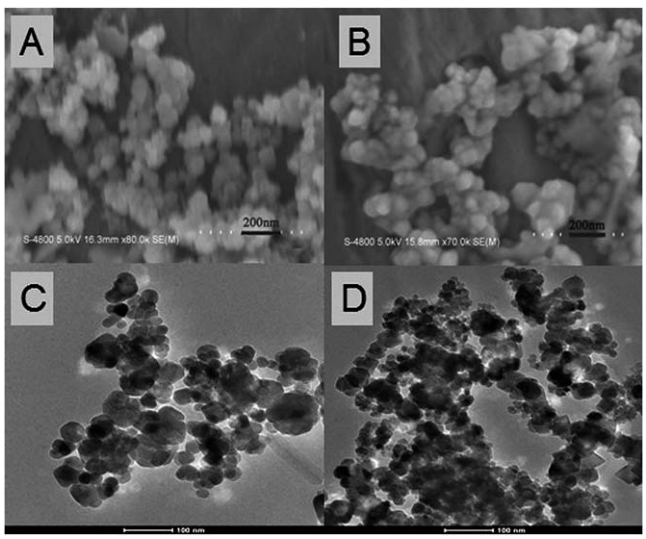

Fig. 2 SEM images of Fe NPs (A) and Fe@Au NPs (B); TEM images of Fe NPs (C) and Fe@Au NPs (D).

The influence of Fe@Au NPs on fluorescent intensity

This DNA fluorescent biosensor was fabricated based on the Fe@Au NPs. To find out the optimal concentration of the Fe@Au NPs, different nanoparticles concentrations and 1.0×10^{-6} M MB as the fluorescent probe were examined. As shown in Fig. 3A, there is quenching effect on the fluorescence of MB in the presence of the Fe@Au NPs. The fluorescent intensity of MB decreased as the concentration of Fe@Au NPs increased. On the other hand, if the concentration of the nanoparticles was very low, less DNA could immobilize on the nanoparticles, and hence the sensitivity of the DNA detection was lower. From the point of view of sensitivity, we selected 0.2 mg mL^{-1} as the concentration of the nanoparticles. In addition, to find out whether the MB can bind to the nanoparticles or not, a contrast experiment was performed. Fe@Au NPs or probe DNA functionalized Fe@Au NPs were added to 2.0 mL of 0.01 M Tris-HCl solution containing 1.0×10^{-5} M MB and incubated for 20 min. And then the fluorescence intensity was detected and the results are shown in Fig. 3B. From Fig. 3B, it is obvious that MB could not bind to the nanoparticles directly.

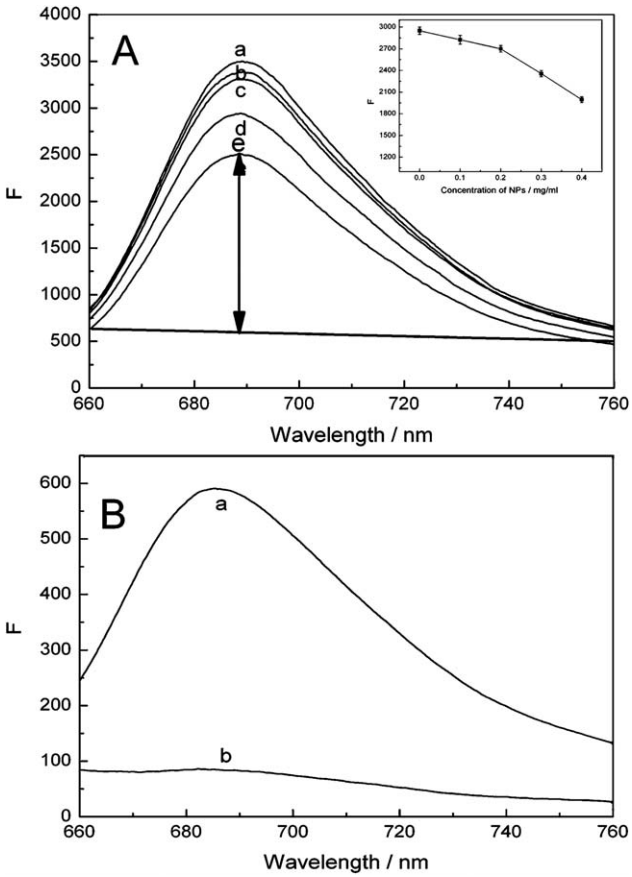

Fig. 3 (A) Fluorescence spectra of 1.0×10^{-6} M MB in the absence (a) and presence of different concentrations of Fe@Au nanoparticles: 0.1 mg mL^{-1} (b), 0.2 mg mL^{-1} (c), 0.3 mg mL^{-1} (d) and 0.4 mg mL^{-1} (e). Inset: Plot of fluorescent signal of MB *vs.* concentrations of Fe@Au NPs. (B) Fluorescence spectra of probe DNA functionalized Fe@Au NPs (a) and Fe@Au NPs (b).

Optimization of DNA assay conditions

In this work, the effect of assay conditions on the experimental results (such as pH, hybridization time and accumulation time of MB) was investigated (Fig. 4). From Fig. 4A it is obviously observed that the fluorescent intensity of MB increased with the increase of solution pH from 6.40 to 7.40, then decreased when the pH is greater than 7.40. From Fig. 4B, it is clearly observed that the change of fluorescent intensity (ΔF) increased with the increase of hybridization time from 10 to 30 min, then it remained constant over 30 min. As seen from Fig. 4C and 4D, both accumulation time and ionic strength affected the fluorescent intensity. According to the results as shown in Fig. 4, the optimization of DNA assay conditions are as follows: the buffer solution pH is 7.40, hybridization time is 30 min, the MB accumulation time is 20 min and 0.20 M NaCl were selected.

The selectivity of the DNA detection

The selectivity of this biosensor was tested using probe DNA functionalized Fe@Au NPs to hybridize with non-complementary sequence (A), one-base mismatched sequence (B) and complete complementary sequence (C) (1.0×10^{-10} M) and the

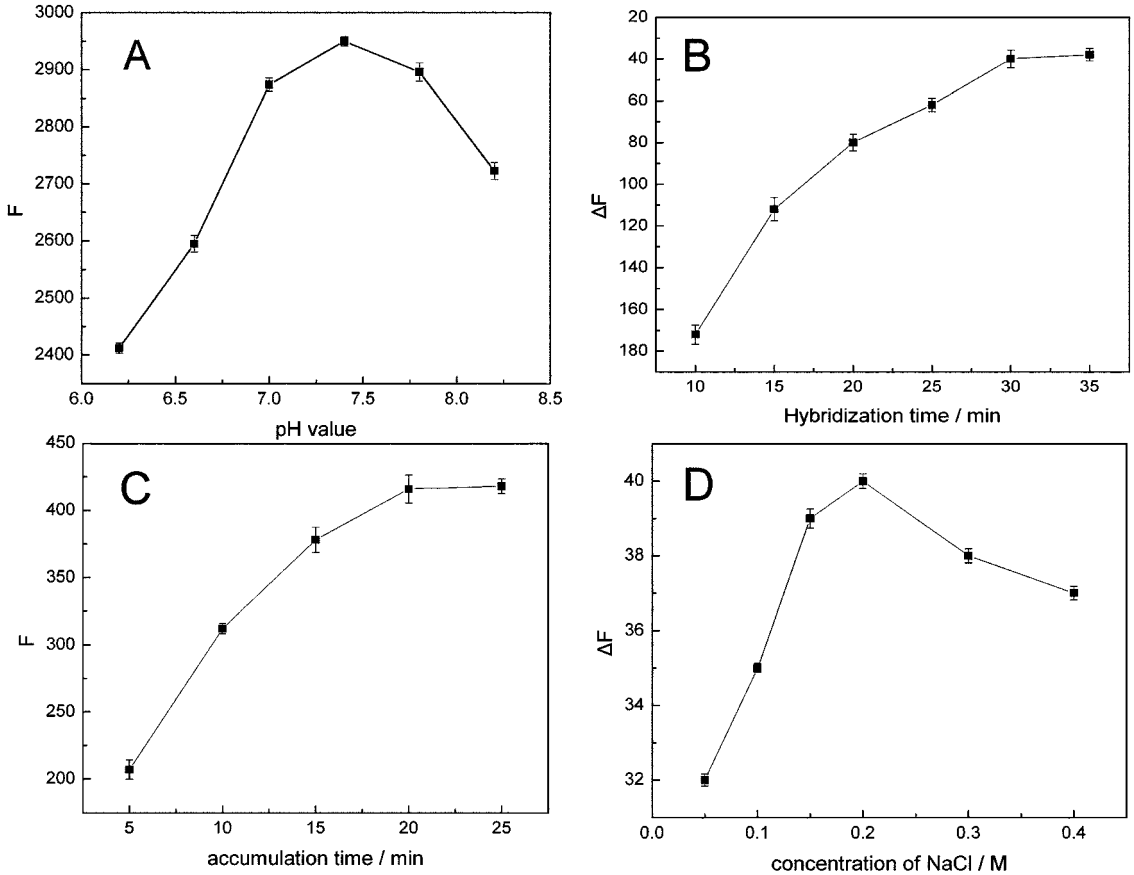

Fig. 4 (A) Effect of pH on fluorescence intensity of MB ($C_{MB} = 1.0 \times 10^{-6}$M). (B) Effect of accumulation time on the fluorescence intensity of MB ($C_{MB} = 1.0 \times 10^{-5}$M). (C) The decrease of the fluorescence intensity dependence of DNA hybridization time ($C_{complementary\ DNA} = 1.0 \times 10^{-10}$ M). (D) Effect of ionic strength on the DNA hybridization ($C_{complementary\ DNA} = 1.0 \times 10^{-10}$ M; NaCl concentration: 0.05, 0.10, 0.15, 0.20, 0.30, 0.40 M).

results are shown in Fig. 5. It could be clearly observed that the fluorescence intensity of the non-complementary sequence is the lowest. Also, a smaller decrease in values was obtained when the probe DNA hybridized with one-base mismatched sequence. This could be ascribed to the fact that the one-base mismatched sequence can not fully hybridize with the probe DNA. However, the complete complementary sequence gave the largest response because fewer MB molecules could bind to ds-DNA than ss-DNA. These results showed that this biosensor could distinguish the one-base mismatched sequence.

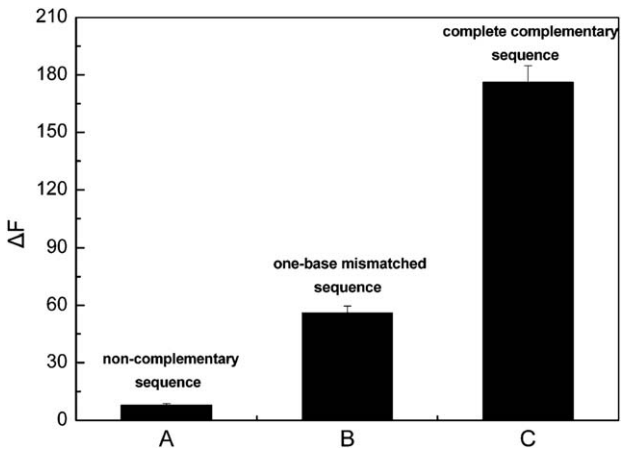

Fig. 5 Histograms of the decrease of fluorescence intensity ($\Delta F = F_{ssDNA} - F_{dsDNA}$) at different DNA sequences: (A) non-complementary sequence; (B) one-base mismatched sequence; (C) complete complementary sequence (concentration: 1.0×10^{-10} M).

Analytical performance

Under the optimal conditions, the probe DNA functionalized Fe@Au NPs were used to hybridize with the different concentrations of complementary DNA (Fig. 6). It could be observed that the fluorescence intensity of MB decreased with the increase of complementary target DNA concentrations. The decreased values of fluorescence intensity (ΔF) were linearly decreased with complementary target DNA concentration from 3.0×10^{-13} to 1.0×10^{-9} M. The regression equation was $\Delta F = 67.8278 \log C_{DNA} + 852.1188$ (unit of C is M), and the regression coefficient (R) of the linear curve was 0.9942. The detection limit for complementary DNA was estimated at 1.0×10^{-13} M (S/N = 3).

We have consulted some literatures which used the fluorescence technique to detect target DNA. From the view of the analysis method, linear range and sensitivity, we compared this work with published papers. The data are shown in Table 1, indicting that the proposed method has the advantages over other literature reports.[30–34]

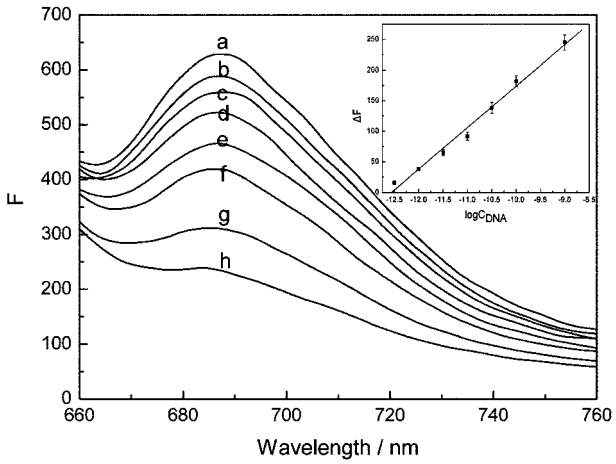

Fig. 6 Representative fluorescence spectra for the probe DNA hybridized with various concentrations of complementary DNA: (a) 0 M; (b) 3.0×10^{-13} M; (c) 1.0×10^{-12} M; (d) 3.0×10^{-12} M; (e) 1.0×10^{-11} M; (f) 3.0×10^{-11} M; (g) 1.0×10^{-10} M; (h) 1.0×10^{-9} M. Inset: Logarithmic plot for signal *versus* target DNA. Signal was defined as the decrease of fluorescence intensity before and after hybridization ($\Delta F = F_{ssDNA} - F_{dsDNA}$). Error bars show the standard deviations of measurements taken from at least three independent experiments. Accumulation time of MB: 20 min; hybridization time: 30 min.

Real samples assay

In order to test the applicability of the proposed method, we selected rabbit blood (samples 1, 2) and human blood (samples 3, 4) as real samples. The fresh blood was first prepared by centrifugation for 5 min at 10 000 rpm, and then the upper solution was collected and used as the hybridization solution. The hybridization and detection followed the steps in the section of 'Hybridization and fluorescence detection'. The results are shown in Table 2. From Table 2, it could be observed that the recovery was about 85%. The reason may be ascribed to the fact that the hybridization solution was taken from upper solution of the blood and the magnetic separation was not completed (*e.g.* adsorption, *etc.*), and consequently the recovery would be lower than 100%. However, it can also meet the need of analysis. So it is posssible for this biosensor to be used for real samples analysis.

Table 1 Comparison of various fluorescence DNA detection methods

The analytical methods of DNA detection	Linear range/nM	Detection limit/nM	Reference
DNA detection using core/shell CdSe/ZnS nanocrystals–DNA conjugates	10–50	2	30
Fluorescence quenching between gold NPs–DNA and carboxytetramethylrhodamine–DNA	1.4–92	2	31
Fluorescence quenching between gold NPs and DNA–fluorescein based on DNA ligase reaction	1–10	0.3	32
DNA detection based on ssDNA, target DNA and dye-doped nanoparticle/DNA conjugates	0.005–10	0.001	33
Fluorescence detection based on magnetic luminescent NPs–DNA conjugates and DNA–Alexa	0.001–0.5	—	34
Fluorescence detection based on Fe/Au core/shell NPs–DNA and MB in solution	0.0003–1	0.0001	This paper

Table 2 Results of determination of target DNA in blood samples

Sample no.	DNA detected/M ($n = 5$)	DNA added/M	DNA found/M ($n = 5$)	Recovery (%) ($n = 5$)
1	0	1.0×10^{-10}	8.5×10^{-11}	85
2	0	1.0×10^{-11}	8.3×10^{-12}	83
3	0	1.0×10^{-10}	8.3×10^{-11}	83
4	0	1.0×10^{-11}	8.7×10^{-12}	87

Conclusions

We have presented a sensitive fluorescent DNA biosensor based on Fe@Au NPs. And this biosensor exhibited higher sensitivity and selectivity, even for single-mismatched DNA detection. The change of fluorescence intensity of MB (ΔF) was linear with the concentration of the complementary DNA from 3.0×10^{-13} to 1.0×10^{-9} M with a detection limit of 1.0×10^{-13} M (S/N = 3). In particular, the proposed method had been successfully used for real samples, and the recovery is about 85%.

Acknowledgements

We gratefully acknowledge the National Nature Science Foundation of China (No. 20675002), which financially supported this work.

References

1 F. Pâques and P. Duchateau, *Curr. Gene Ther.*, 2007, **7**, 49–66.
2 R. Meyer, *Food Control*, 1999, **10**, 391–399.
3 Y. Liu-Stratton, S. Roy and C. K. Se, *Toxicol. Lett.*, 2004, **150**, 29–42.
4 J. Zhang, R. J. Lao, S. P. Song, Z. Y. Yan and C. H. Fan, *Anal. Chem.*, 2008, **80**, 9029–9033.
5 M. Y. Li, S. S. Huang, P. S. Zhu, L. M. Kong, B. Peng and H. Gao, *Electrochim. Acta*, 2009, **54**, 2284–2289.
6 V. Benoit, A. Steel, M. Torres, Y. Y. Yu, H. J. Yang and J. Cooper, *Anal. Chem.*, 2001, **73**, 2412–2420.
7 R. Y. Wang, M. N. Ji, R. Q. Wang and J. Shi, *Spectrochim. Acta, Part A*, 2008, **71**, 1042–1048.
8 S. W. Bae, J. W. Oh, I. S. Shin, M. S. Cho, Y. R. Kim, H. Kim and J. I. Hong, *Analyst*, 2010, **135**, 603–607.
9 K. Aslan, S. N. Malyn, G. Bector and C. D. Geddes, *Analyst*, 2007, **132**, 1122–1129.
10 F. He, F Feng, X. Duan, S. Wang, Y. Li and D. Zhu, *Anal. Chem.*, 2008, **80**, 2239–2243.
11 A. G. Frutos, S. Pal, M. Quesada and J. Lahiri, *J. Am. Chem. Soc.*, 2002, **124**, 2396–2397.
12 J. Bohm, A. Hahn, R. Schubert, G. Bahnweg, N. Adler, J. Nechwatal, R. Oehlmann and W. Obwald, *J. Phytopathol.*, 1999, **147**, 409–416.
13 X. L. Mao, L. J. Yang, X. L. Su and Y. B. Li, *Biosens. Bioelectron.*, 2006, **21**, 1178–1185.
14 X. W. Tang, S. Bansaruntip, N. Nakayama, E. Yenilmez, Y. L. Chang and Q. Wang, *Nano Lett.*, 2006, **6**, 1632–1636.
15 L. Zeng, K. K. Luo and Y. F Gong, *J. Mol. Catal. B: Enzym.*, 2006, **38**, 24–30.
16 A. K. Gupta, R. R. Naregalkar, V. D. Vaidya and M. Gupta, *Nanomedicine*, 2007, **2**, 23–39.

17 E. Palecek and M. Fojta, *Talanta*, 2007, **74**, 276–290.
18 S. A. M. Martins, D. M. F. Prazeres, L. P. Fonseca and G. A. Monteiro, *Anal. Biochem.*, 2009, **391**, 17–23.
19 M. Pita, J. M. Abad, C. Vaz-Dominguez, C. Briones, E. Mateo-Martí, J. A. Martín-Gago, M. P. Morales and V. M. Fernández, *J. Colloid Interface Sci.*, 2008, **321**, 484–492.
20 G. N. Wang and X. G. Su, *Anal. Bioanal. Chem.*, 2010, **397**, 1251–1258.
21 N. Zammatteo, I. Alexandre, I. Ernest, L. Le, F. Brancart and J. Remacle, *Anal. Biochem.*, 1997, **253**, 180–189.
22 H. Kuhn, V. V. Demidov, J. M. Coull, M. J. Fiandaca, B. D. Gildea and M. D. Frank-Kamenetskii, *J. Am. Chem. Soc.*, 2002, **124**, 1097–1103.
23 N. J. Parham, F. J. Picard, R. Peytavi, M. Gagnon, G. Seyrig, P. Gagné, M. Boissinot and M. G. Bergeron, *Clin. Chem.*, 2007, **53**, 1570–1576.
24 T. J. Legler, Z. Liu, K. H. Heermann, M. Hempel, K. Gutensohn, H. Kiesewetter and A. Pruss, *Transfus. Apheresis Sci.*, 2009, **40**, 153–157.
25 A. Son, D. Dosev, M. Nichkova, Z. Y. Ma, I. M. Kennedy, K. M. Scow and K. R. Hristova, *Anal. Biochem.*, 2007, **370**, 186–194.
26 G. K. Kouassi and J. Irudayaraj, *Anal. Chem.*, 2006, **78**, 3234–3241.
27 W. R Yang, M. Ozsoz, D. B. Hibbert and J. J. Gooding, *Electroanalysis*, 2002, **14**, 1299–1302.
28 R. Rohs, H. Sklenar, R. Lavery and B. Ro1der, *J. Am. Chem. Soc.*, 2000, **122**, 2860–2866.
29 J. Lin, W. L. Zhou, A. Kumbhar, J. Wiemann, J. Y. Fang, E. E. Carpenter and C. J. O'Connor, *J. Solid State Chem.*, 2001, **159**, 26–31.
30 D. Gerion, F. Q. Chen, B. Kannan, A. H. Fu, W. J. Parak, D. J. Chen, A. Majumdar and A. P. Alivisatos, *Anal. Chem.*, 2003, **75**, 4766–4772.
31 Z. S. Wu, J. H. Jiang, L. Fu, G. L. Shen and R. Q. Yu, *Anal. Biochem.*, 2006, **353**, 22–29.
32 H. Wang, J. S. Li, Y. X. Wang, J. Y. Jin, R. H. Yang, K. M. Wang and W. H. Tan, *Anal. Chem.*, 2010, **82**, 7684–7690.
33 X. C. Zhou and J. Z. Zhou, *Anal. Chem.*, 2004, **76**, 5302–5312.
34 A. Son, A. Dhirapong, D. K. Dosev, I. M. Kennedy, R. H. Weiss and K. R. Hristova, *Anal. Bioanal. Chem.*, 2008, **390**, 1829–1835.